Supporting Information

Transformation and sorption of illicit drug biomarkers in sewer biofilms

Pedram Ramin[a,b*], Andreas Libonati Brock[a], Ana Causanilles[c], Borja Valverde-Pérez[a], Erik Emke[c], Pim de Voogt[c,d], Fabio Polesel[a], Benedek Gy. Plósz[a,e,*]

[a]Department of Environmental Engineering, Technical University of Denmark (DTU), Bygningstorvet, Bygning 115, 2800 Kgs. Lyngby, Denmark

[b]Process and Systems Engineering Center (PROSYS), Department of Chemical and Bio-chemical Engineering, Technical University of Denmark, Building 229, 2800 Kgs. Lyngby, Denmark

[c]KWR Watercycle Research Institute, P.O. Box 1072, 3430 BB Nieuwegein, The Netherlands

[d]Institute for Biodiversity and Ecosystem Dynamics, University of Amsterdam, P.O. Box 94248, 1090 GE Amsterdam, The Netherlands

[e]Department of Chemical Engineering, University of Bath, Claverton Down, Bath BA2 7AY,UK

**Corresponding authors*: pear@kt.dtu.dk; b.g.plosz@bath.ac.uk

Number of pages: 17

Number of figures: 12

Number of tables: 4

Calculation of dimensionless numbers

Sherwood number (*Sh*) was approximated using the empirical formulation suggested by Strong and Carlucci[1]:

$$Sh = \frac{k_b d_p}{D_w} = 0.0017 Sc^{1.502} (T_a/T_{ac})^{0.36} \qquad \text{(eq. S1)}$$

In which *Sc* is the Schmidt number:

$$Sc = \frac{\nu}{D_w} \qquad \text{(eq. S2)}$$

Where ν (m^2 s^{-1}) is the kinematic viscosity of water (1.07×10^{-6} m^2 s^{-1}) and D_w (m^2 d^{-1}) is the Diffusion coefficient (Table S1). k_b (m d^{-1}) is the mass transfer coefficient between bulk phase and the biofilm (k_b=D_w/L_b). The characteristic length, d_p (m), is considered as 2(R_2-R_1).[2] Where R_1 (0.045 m) and R_2 (0.057 m) are respectively the radius of inner and outer cylinder.

In eq. S1. T_a is the Taylor number and T_{ac} is the critical Taylor number as an instability threshold for flow in the gap between two cylinders.[3] T_a is defined as[4]:

$$T_a = \frac{1-R_2/R_1}{R_2/R_1}\left(\frac{\Omega R_1 d}{\nu}\right)^2 \qquad \text{(eq. S3)}$$

Ω is the angular velocity (2.1 rad s^{-1}) and *d* is the gap between two cylinders (R_2-R_1). Recktenwald et al.[4] evaluted the T_{ac} values for a range of radius ratios (R_2/R_1) and axial Reynolds number. Axial Reynolds number was calculated according to:

$$Re = \frac{\bar{u} d_p}{\nu} \qquad \text{(eq. S4)}$$

Where $\bar{u}$ (m d^{-1}) is the average axial velocity (1.2×10^{-5} m s^{-1} during batch experiment and 28.9×10^{-5} m s^{-1} during continuous operation).

Based on the operational condition of the reactors during 2 d batch experiments, T_a and T_{ac} estimated as 2.98×10^5 and 2.32×10^3 and Reynolds number was 6.48. During continuous operation, Reynolds number was 0.3 and T_{ac} was 2.24×10^3.

Since T_a was higher than T_{ac} it can be expected that instability and Taylor vortices would occur inside the reactors. Based on these dimensionless numbers and their correlation according to Recktenwald et al.[4], the flow pattern in the reactors was in between *absolutely stable* and *convectively unstable* regions.

Table S1. Molecular weight, molar volume[5] and diffusion coefficients for selected drug biomarkers

Compound	Molecular weight	Molar volume (cm^3 mol^{-1})	D_w (m^2 d^{-1})
MEPH	177.24	179.4	4.90×10^{-5}
METD	309.45	306.4	3.58×10^{-5}
EDDP	277.41	263.7	3.91×10^{-5}
COC	303.35	248	4.05×10^{-5}
BE	289.33	223.1	4.31×10^{-5}
EME	199.25	168.6	5.09×10^{-5}
CE	317.38	264.2	3.90×10^{-5}
HER	369.41	273.6	3.82×10^{-5}
6MAM	327.37	235.7	4.17×10^{-5}
MORG	461.46	279.7	3.77×10^{-5}
MOR	285.34	197.6	4.63×10^{-5}
COE	299.36	222.6	4.32×10^{-5}
NCOE	285.34	207.5	4.50×10^{-5}
THC	314.46	309.7	3.55×10^{-5}
THCOH	330.46	308.3	3.56×10^{-5}
THCCOOH	344.44	301.9	3.61×10^{-5}

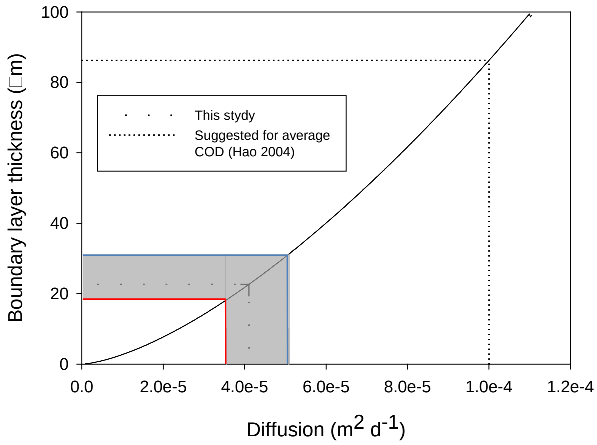

Figure S1. Boundary layer thickness as a function of diffusion, according to eq. S1 and eq. S2. In this study an average diffusion of all drug biomarkers (4.11×10^{-5} m^2 d^{-1}) was used to estimate an averaged boundary layer thickness (22 µm). This thickness is approximately 4 times lower than the boundary layer for typical COD in the sewage (86 µm), assuming an averaged diffusion of (1×10^{-4} m^2 d^{-1}).[6] Among the selected drug biomarkers THC has the lowest diffusivity (3.55×10^{-5} m^2 d^{-1}), which corresponds to the boundary layer of 18.23 µm (red line), and EME has the highest diffusion coefficient (5.09×10^{-5} m^2 d^{-1}), which corresponds to the boundary layer of 31.22 µm (blue line). The gray shaded area covers the range of boundary layer values and corresponding to diffusion coefficients of the chemicals selected in this study.

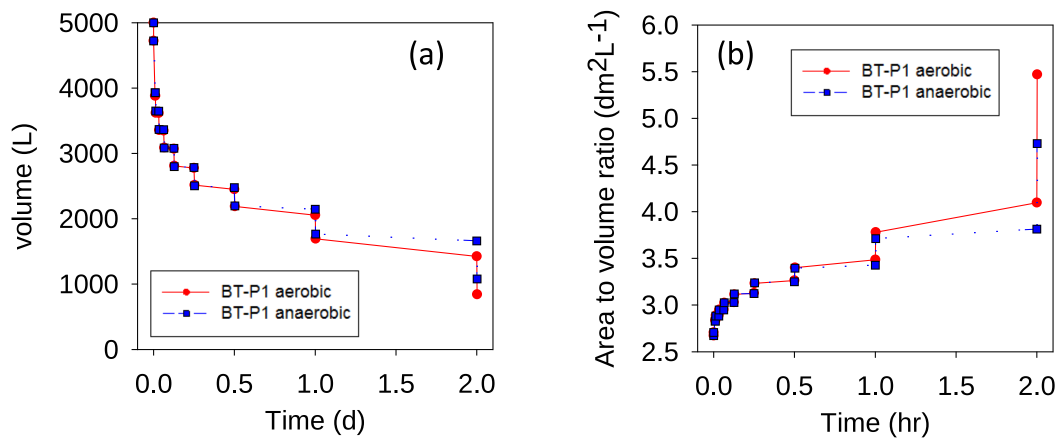

Figure S2. The variation of volume (a) and area to volume ratio (b) in external tanks during BT-P1 aerobic and anaerobic experiments. The variations are due to sample withdrawal during experiments. Same variations were considered for BT-P2 experiments. These variations were used to simulate the dynamics of the volume of the external tanks as well as partitioning of drug biomarkers onto tank wall.

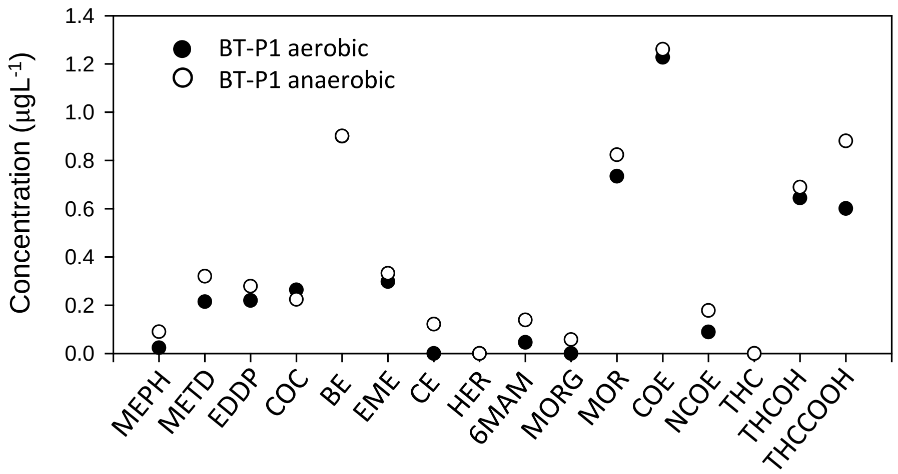

Figure S3. Background concentration of drug biomarkers during BT-P1 aerobic and an-aerobic experiments. Targeted internal standard compounds (spiked at 10 µg L^{-1}) were considerably higher than the background concentrations.

Table S2. List of batch experiments including measurements for TSS and VSS (based on duplicates), as well as pH and temperature (reported as mean ± standard deviation, measured throughout experiments). Experiment AB-SO is identical to our previous study.[7] Measurements are performed inside the external tank.

Experiment ID	To assess	Medium type	Duration (h)	Initial volume (L)	TSS (mgL^{-1})	VSS ($mg\ L^{-1}$)	pH	T (°C)
BT-P1 aerobic	Biotransformation using procedure 1	Centrifuged and filtered pre-clarified wastewater	48	5	42.4	37.5	8.82± 0.05	14.89± 0.34
BT-P1 anaerobic	Biotransformation using procedure 1	Centrifuged and filtered pre-clarified wastewater	48	5	103.75	46.25	9.49 ± 0.23	16.25± 0.41
BT-P2 aerobic	Biotransformation using procedure 2	Centrifuged and filtered pre-clarified wastewater	48	5	91.7	26	8.80± 0.06	15.30± 0.64
BT-P2 anaerobic	Biotransformation using procedure 2	Centrifuged and filtered pre-clarified wastewater	48	5	80	20	8.72 ± 0.19	16.03± 0.64
SO1	Sorption to aerobic biofilm	Suspended biofilm biomass, NaN_3	4	4	63.75	46.25	7.91± 0.08	15.38± 0.18
SO2	Sorption to anaerobic biofilm	Suspended biofilm biomass, NaN_3	4	4	95	68.75	7.91± 0.08	15.32± 0.13
AB-SO	Control for SO1 and SO2	Mineral water, NaN_3	4	4	0	0	7.91± 0.12	14.82± 0.23

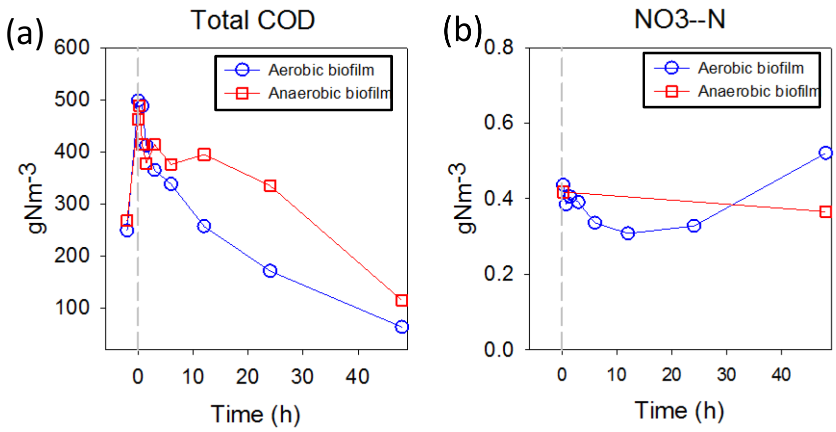

Figure S4 Measurements of total COD (a), nitrate nitrogen ($NO3^{-}$-N) (b) during BT-P1 experiments. Measurements before t=0 are related to the samples taken prior to spiking of standards. Lines connecting data points are based on simple linear interpolation to show the trends.

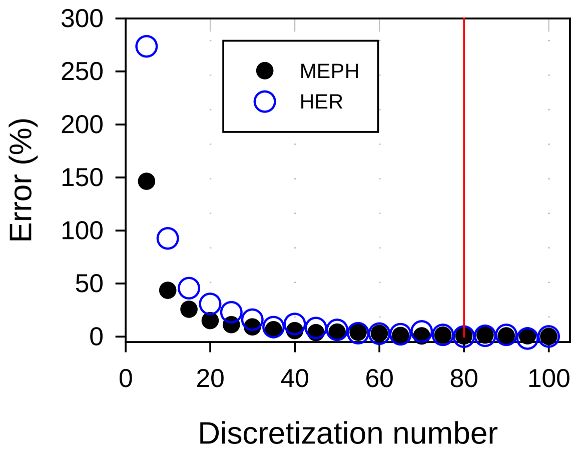

Figure S5. The impact of biofilm model discretization number (number of grid points) on estimation of k_f (d^{-1}) presented as error percentage. The error is calculated for aerobic transformation rates of MEPH and HER by comparing the estimations with the reference scenarios (i.e. 100 grid points) for each of the compounds. In this study, 80 grid points are considered to be sufficient as the error became independent from the discretization number.

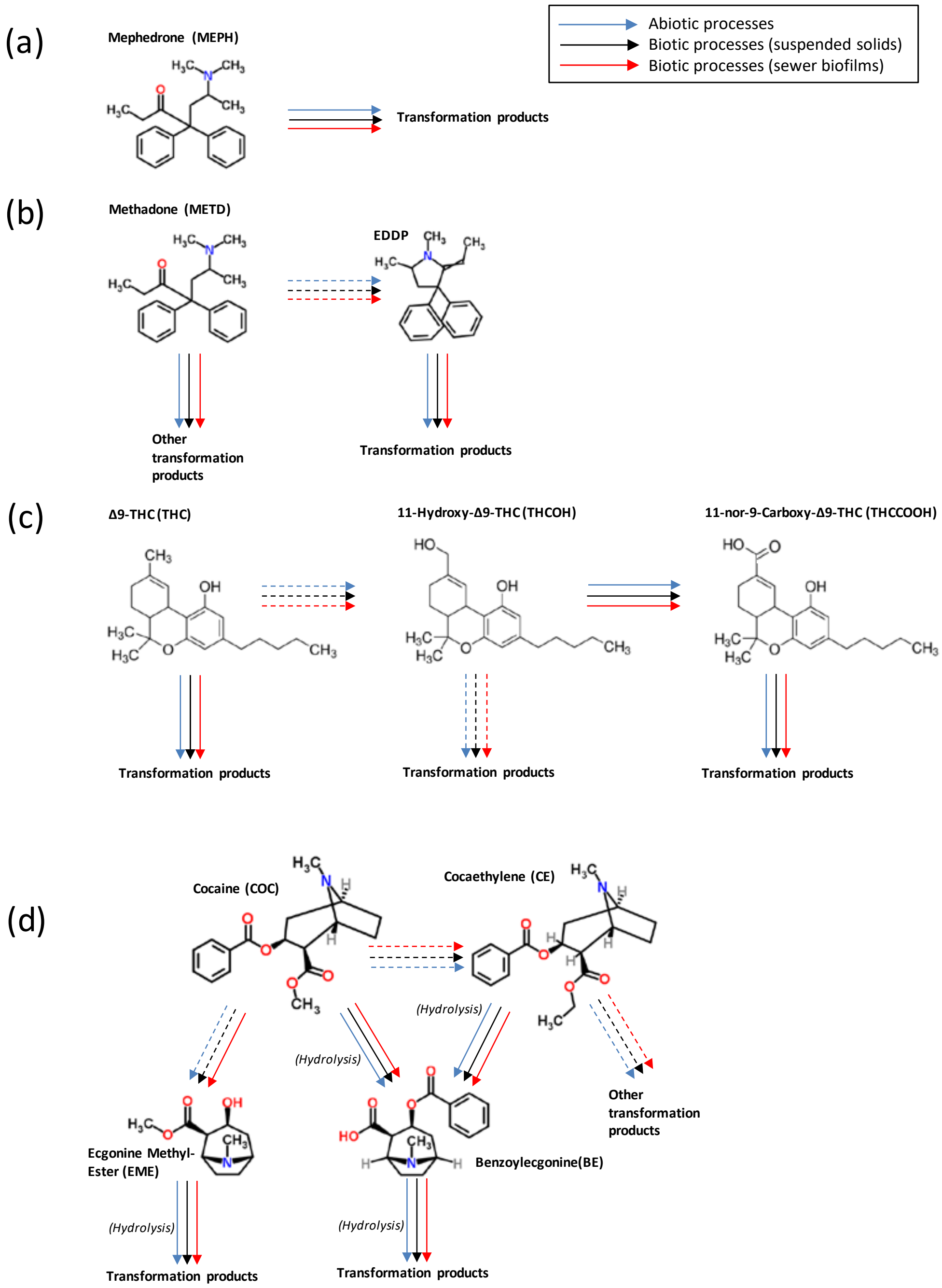

Figure S6. Transformation pathway of MEPH (a), METD and EDDP (b), THC, THCOH and THCCOOH (c) and COC, BE, EME and CE (d). Blue and black arrows indicate abiotic and biotic processes due to suspended solids.[7] Red arrows indicate sewer biofilm-mediated transformations. Dashed arrows are considered as minor transformations.

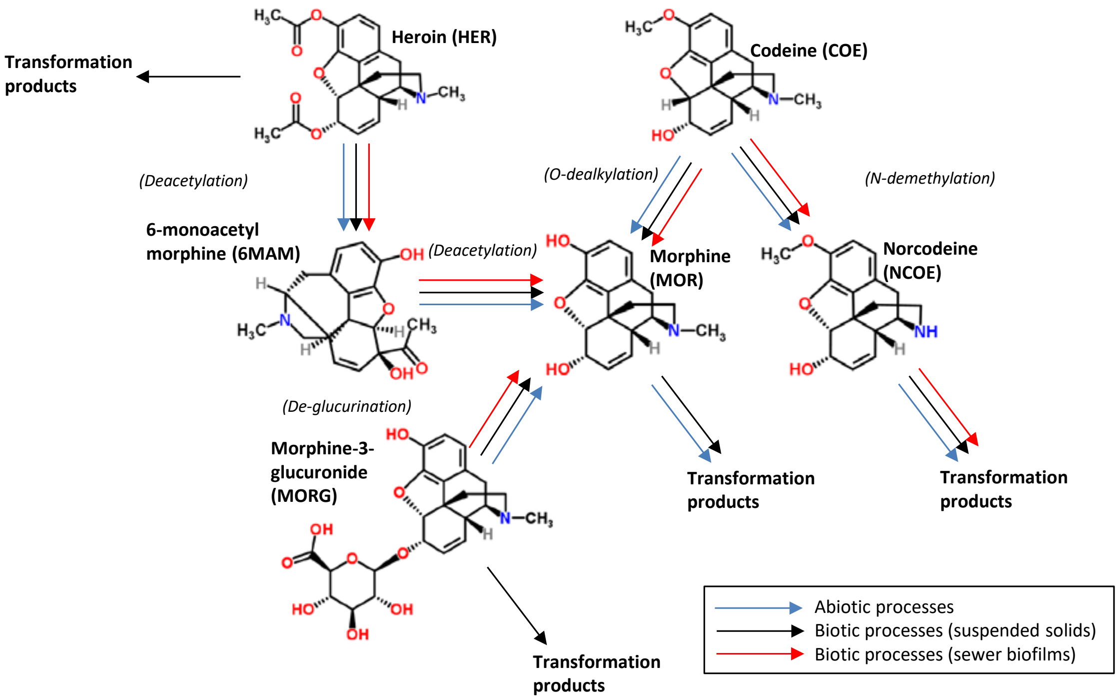

Figure S7. Transformation pathway of HER and its transformation products, 6MAM and MOR including its human metabolite MORG. The pathway also include COE and NCOE. Blue and black arrows indicate abiotic and biotic processes due to suspended solids.[7] Red arrows indicate sewer biofilm-mediated transformations.

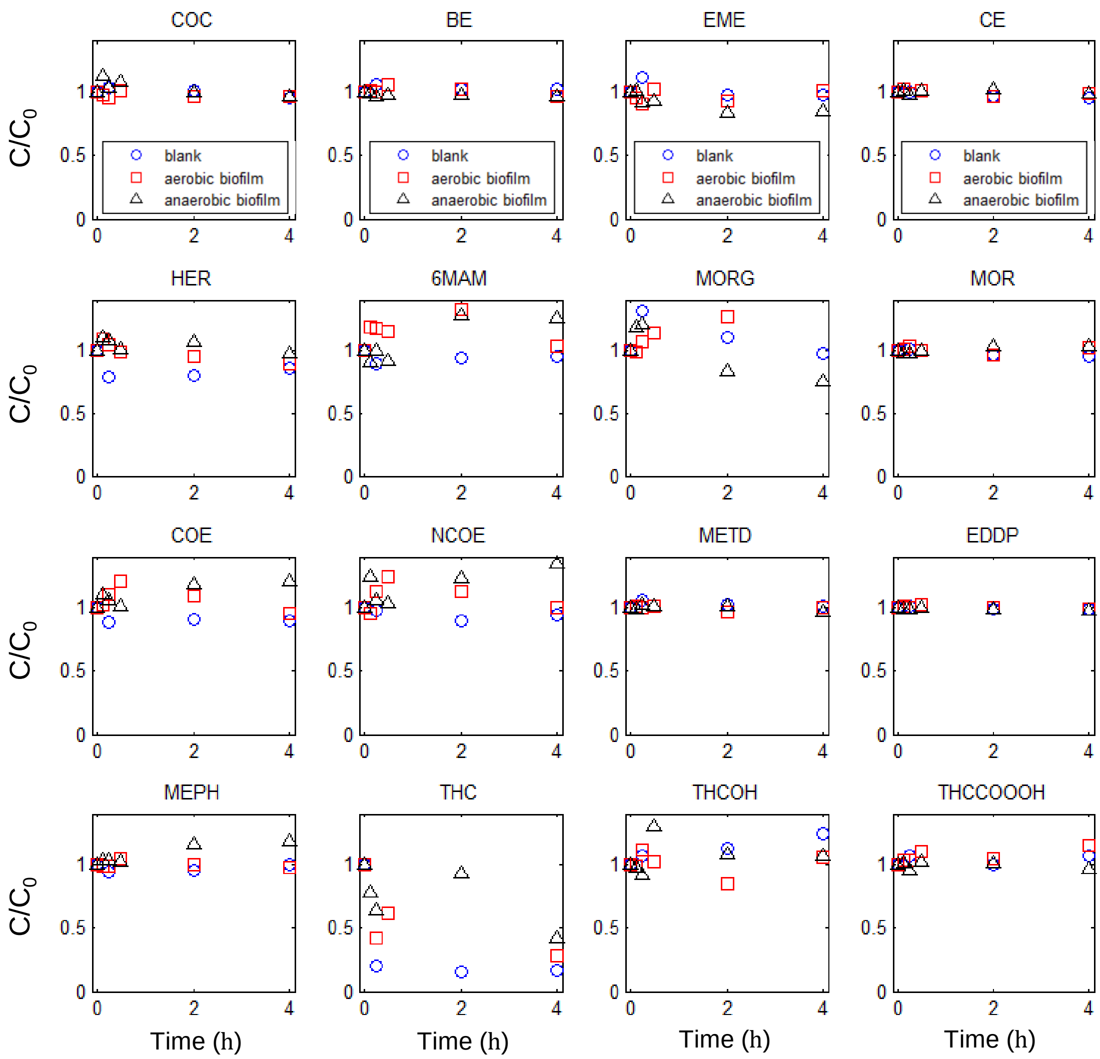

Figure S8. Normalized concentration of selected drug biomarkers during sorption experiments with aerobic and anaerobic biofilms (SO1 and SO2 respectively). Blank data are related to AB-SO experiment (data from Ramin et al.[7]), indicated by blue circles. SO1 and SO2 data are shown with red squares and black triangles respectively.

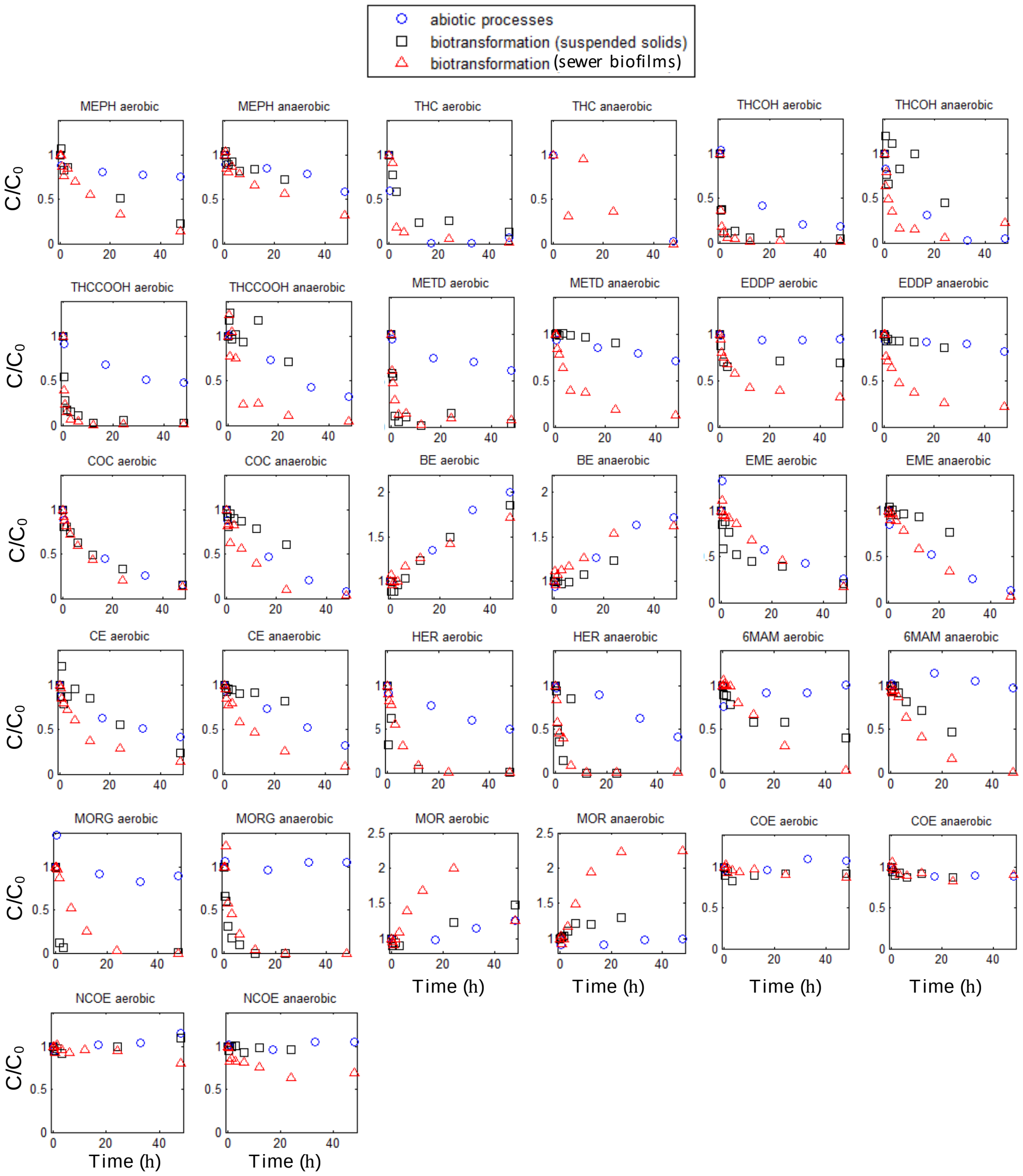

Figure S9. Normalized concentration of selected drug biomarkers during various experiments under aerobic and anaerobic conditions. i) blank experiment using mineral water to assess abiotic processes indicated by blue circles (data from Ramin et al.[7]); ii) transformation of drug biomarkers in raw wastewater indicated by black squares (data from Ramin et al.[7]); iii) sewer biofilms-mediated transformation of drug biomarkers indicated by red triangles (this study).

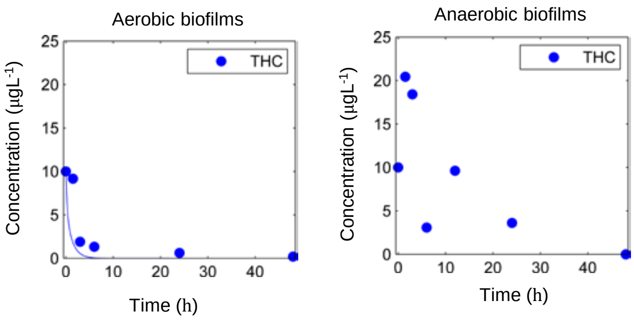

Figure S10. Concentration of THC during BT-P1 experiment (marks). In aerobic biofilm, simulation (line) was done with $k_{biof,ae,THC}$=0 as all removal was attributed to abiotic process. Due to lack of estimated $k_{abio,an,THC}$ (d^{-1}) and $k_{bio,an,THC}$ (L $gTSS^{-1}$ d^{-1}) for THC in literature, no simulation was possible for this compound under anaerobic conditions.

Table S3. Estimated partitioning coefficients to tank wall, K_{dw} (L dm^{-2}) and suspended solids, K_d (L gTSS^{-1}) abiotic transformation rate, k_{abio} (d^{-1}), and biotransformation rate for suspended solids, k_{bio} (L gTSS^{-1} d^{-1}) under aerobic and anaerobic conditions. All these values are reported by Ramin et al.[7], except the values for HER, COE and their human metabolites, under anaerobic conditions, which are reported by Ramin et al.[8] Transformation rates are presented as median ± 95% credibility interval (lower bound, upper bound). Abbreviation: T.P. = transformation product(s).

Compounds	**Transformation**	K_{dw} **(L dm^{-2}) Aerobic tank**	K_{dw} **(L dm^{-2}) Anaerobic tank**	K_d **(L gTSS^{-1}) Aerobic tank**	K_d **(L gTSS^{-1}) Anaerobic tank**	$k_{abio,ae}$ **(d^{-1}) Aerobic**	$k_{abio,an}$ **(d^{-1}) Anaerobic**	$k_{bio,ae}$ **(L gTSS^{-1}d^{-1}) Aerobic**	$k_{bio,an}$ **(L gTSS^{-1}d^{-1}) Anaerobic**
MEPH	MEPH→T.P.	0.04	0.04	0	0.25	0.10 (0.07, 0.15)	0.18 (0.10, 0.31)	1.86 (1.54, 2.19)	0
METD	METD→T.P.	0.02	0.02	0.11	0	0.25 (0.20, 0.31)	0.15 (0.13, 0.17)	86.87 (59.26, 151.71)	0
EDDP	EDDP→T.P.	0.01	0.03	0.16	0.03	0.03 (0.01, 0.05)	0.06 (0.03, 0.11)	0.74 (0.13, 2.26)	0.05 (0.00, 0.17)
COC	COC→BE	0.04	0.05	0	0	1.03 (0.94, 1.14)	1.15 (0.98, 1.36)	0.70 (0.06, 2.26)	0
	COC→EME					0	0	0	0
BE	BE→T.P.	0.003	0.03	0.12	0	0.13 (0.04, 0.33)	0.19 (0.08, 0.57)	0.26 (0.01, 1.44)	1.97 (0.10, 12.88)
EME	EME→T.P.	0	0.06	0	0	0.68 (0.60, 0.77)	0.97 (0.81, 1.20)	2.66 (0.68, 7.94)	0
CE	CE→BE	0.05	0.02	0	0	0.45 (0.37, 0.52)	0.49 (0.39, 0.62)	0.37 (0.02, 1.30)	0
HER	HER→ 6MAM	0.03	0.01	0	0	0.32 (0.28, 0.36)	0.35 (0.23, 0.56)	5.65 (0.19, 17.93)	15.06 (2.92, 33.61)
	HER→ T.P.					0		13.73 (1.48, 19.32)	38.05 (18.06, 54.89)
6MAM	6MAM→ MOR	0	0	0.64	0.31	0.21 (0.12, 0.32)	0.22 (0.10, 0.35)	2.00 (0.22, 14.80)	2.20 (1.14, 3.75)
MORG	MORG→ MOR	0	0	0	0	0.08 (0.03, 0.15)	0	19.08 (0.55, 89.39)	11.488 (0.722, 55.372)
	MORG→ T.P.					0	0	83.01 (13.58, 114.72)	50.672 (11.328, 78.832)
MOR	MOR→T.P.	0.03	0.03	0	0	0.17 (0.01, 0.85)	0.170 (0.027, 0.705)	0.65 (0.01, 3.78)	1.458 (0.077, 14.718)
COE	COE→NCOE	0.02	0.02	0	0	0	0.044 (0.006, 0.086)	0	0.114 (0.005, 0.393)
	COE→MOR					0	0.026 (0.001, 0.084)	0	0.146 (0.005, 0.423)
NCOE	NCOE→T.P.	0.02	0	0	0.01	0	0.021 (0.001, 0.084)	0	0.246 (0.018, 0.707)
THC	THC→T.P.	0.16	na*	0	0	27.17(12.97, 42.34)	na*	0	na*
THCOH	THCOH→THCCOOH	0	0.07	0	0.75	1.12 (0.83, 1.93)	1.93 (1.45, 3.05)	232.35 (88.51, 884.53)	0
THCCOOH	THCCOOH→ T.P.	0.03	0	0.78	0.80	0.96 (0.73, 1.98)	1.38 (1.15, 2.23)	377.23 (159.88, 920.24)	0

*Undetermined values

Table S4. Estimated partitioning coefficients to biofilm, K_{df} (L $gTSS^{-1}$), sewer-biofilms mediated transformation rate constants, k_{biof} (L $gTSS^{-1}$ d^{-1}), and k'_{biof} (m^3 m^{-2} d^{-1}) in this study. Transformation rate constants are reported as median ± 95% credibility interval (lower bound, upper bound). Abbreviation: T.P. = transformation product(s).

Compounds	Transformation	$k_{df,ae}$ (L $gTSS^{-1}$) Aerobic	$k_{df,an}$ (L $gTSS^{-1}$) Anaerobic	$k_{biof,ae}$ (L $gTSS^{-1}d^{-1}$) Aerobic	$k_{biof,an}$ (L $gTSS^{-1}d^{-1}$) Anaerobic	$k'_{biof,ae}$ (m^3 m^{-2} d^{-1}) Aerobic	$k'_{biof,an}$ (m^3 m^{-2} d^{-1}) Anaerobic
MEPH	MEPH→T.P.	0.20	0	5.88 (4.29, 8.31)	0.08 (0.04, 0.14)	1.69 1.23, 2.39)	0.03 (0.02, 0.06)
METD	METD→T.P.	0.32	0.55	2487.98 (822.67, 3363.13)	183.09 (70.56 .0295)	715.62 (236.63, 967.35)	75.46 (29.08, 197.85)
EDDP	EDDP→T.P.	0	0.15	1.79 (0.45, 6.48)	88.89 (13.01, 702.20)	0.51 (0.13, 1.86)	36.64 (5.36, 289.42)
COC	COC→BE	0	0	0.18 (0.01, 0.54)	0.94 (0.03, 2.9)	0.05 (0.00, 0.16)	0.39 (0.01, 1.20)
	COC→EME			0.26 (0.01, 0.56)	1.63 (0.11, 2.94)	0.07 (0.00, 0.16)	0.67 (0.05, 1.21)
BE	BE→T.P.	0.90	0.62	2.00 (0.07, 10.92)	0.95 (0.06, 5.17)	0.57 (0.02, 3.14)	0.39 (0.02, 2.13)
EME	EME→T.P.	0	1.59	0.05 (0.00, 0.26)	21.03 (0.90, 99.60)	0.02 (0.00, 0.07)	8.67 (0.37, 41.05)
CE	CE→BE	0	0	0.68 (0.36, 1.47)	0.51 (0.24, 1.45)	0.20 (0.10, 0.42)	0.21 (0.10, 0.60)
HER	HER→ 6MAM	0	0	4.43 (2.49, 10.42)	22.14 (4.27, 96.24)	1.28 (0.71, 3.00)	9.13 (1.76, 39.67)
6MAM	6MAM→ MOR	0	0	1.11 (0.54, 3.11)	6.45 (2.25, 26.39)	0.32 (0.15, 0.89)	0.00 (0.00, 0.00)
MORG	MORG→ MOR	0	0	0	2.03 (0.08, 5.42)	0	2.66 (0.93, 10.88)
MOR	MOR→T.P.	0	0	0	0	0	0
COE	COE→NCOE	0	0	0.01 (0.00, 0.03)	0.01 (0.00, 0.01)	0.00 (0.00, 0.01)	0.00 (0.00, 0.01)
	COE→MOR	0	0	0.01 (0.00, 0.03)	0.01 (0.00, 0.01)	0.00 (0.00, 0.01)	0.00 (0.00, 0.01)
NCOE	NCOE→T.P.	0	0	0.04 (0.00, 0.15)	0.20 (0.02, 1.113)	0.01 (0.00, 0.04)	0.08 (0.01, 0.46)
THC	THC→T.P.	0	0	0	na*	0	na*
THCOH	THCOH→THCCOOH	2.81	1.68	21034.16 (6317.54, 28027.67)	5066.29 (1089.14, 15779.5)	6050.11 (1817.13, 8061.67)	2088.13 (448.90, 6503.71)
THCCOOH	THCCOOH→ T.P.	0	1.06	133.07 (20.09, 177.82)	3272.33 (710.94, 10042.8)	38.28 (5.78, 51.15)	1348.73 (293.02, 4139.27)

*Parameter could not be estimated due to unavailable k_{bio}

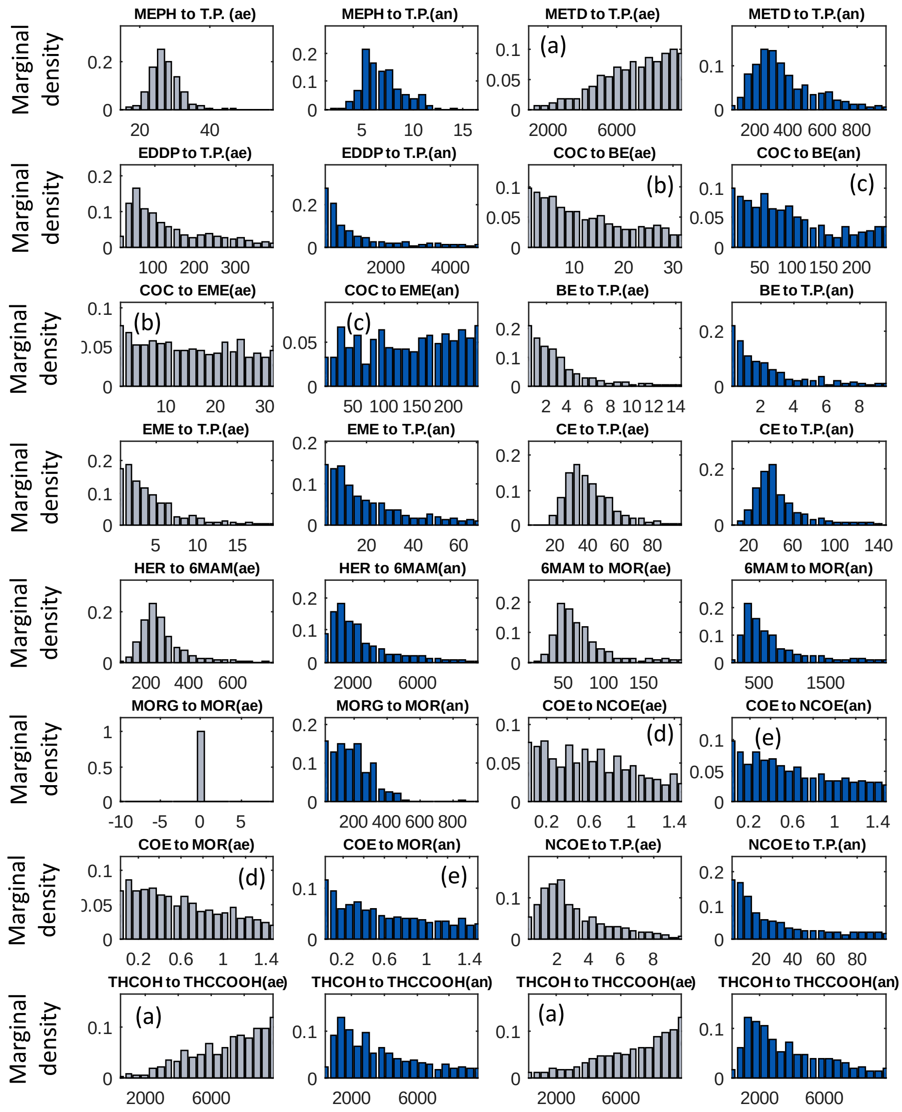

Figure S11 Posterior distribution of estimated parameter, k_f (d^{-1}) = k_{biof} X_{SS}/(1+k_{df} X_{SS}) for aerobic sewer biofilm (gray histograms) and anaerobic sewer biofilm (blue histogram). Abbreviation: ae= aerobic, an= anaerobic, T.P. = transformation product(s).

(a) Distribution is limited by the acceptable upper boundary set at 10^4.
(b) The upper boundary (32.43) of the estimation is limited to the upper boundary of 95% credibility interval initially estimated for total transformation of COC to BE and EME for aerobic sewer biofilm.
(c) The upper boundary (251.59) of the estimation is limited to the upper boundary of 95% credibility interval initially estimated for total transformation of COC to BE and EME for anaerobic sewer biofilm.
(d) The upper boundary (1.49) of the estimation is limited to the upper boundary of 95% credibility interval initially estimated for total transformation of COE to NCOE and MOR for aerobic sewer biofilm.
(e) The upper boundary (1.52) of the estimation is limited to the upper boundary of 95% credibility interval initially estimated for total transformation of COE to NCOE and MOR for anaerobic sewer biofilm.

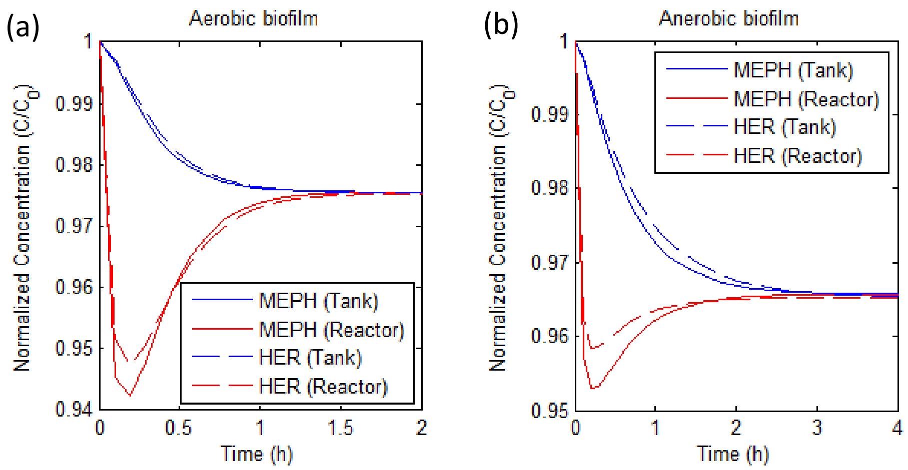

Figure S12. The impact of diffusion into biofilms resulting in concertation drop in the bulk phase in the biofilm reactor (red lines) and in the external tank (blue lines). The simulation results are presented for HER and MEPH normalized concentration in the aerobic (a) and anaerobic (b) biofilms without accounting for partitioning to solids (biofilm and reactor wall) or transformation.

Reference

(1) Strong, A.; Carlucci, L. An experimental study of mass transfer in rotating Couette flow with low axial Reynolds number. *Can. J. Chem. Eng.* **1976**, *5*, 295–298.

(2) Forney, L. J.; Ye, Z.; Koutchma, T. UV Disinfection of E. coli Between Concentric Cylinders: Effects of the Boundary Layer and a Wavy Wall. *Ozone Sci. Eng.* **2008**, *30* (6), 405–412.

(3) Kundu, P. K.; Cohen, I. M.; Dowling, D. R. *Fluid Mechanics*, fifth.; Academic Press, 2012.

(4) Recktenwald, A.; Lücke, M.; Müller, H. W. Taylor vortex formation in axial through-flow: Linear and weakly nonlinear analysis. *Phys. Rev. E* **1993**, *48* (6), 4444–4454.

(5) ACD/I-Lab 2.0 Prediction Software by Advanced Chemistry Development Inc. (ACD/Labs).

(6) Hao, X. Di; van Loosdrecht, M. C. M. Model-based evaluation of COD influence on a partial nitrification-Anammox biofilm (CANON) process. *Water Sci. Technol.* **2004**, *49* (11-12), 83–90.

(7) Ramin, P.; Brock, A. L.; Polesel, F.; Causanilles, A.; Emke, E.; de Voogt, P.; Plósz, B. G. Transformation and sorption of illicit drug biomarkers in sewer systems : understanding the role of suspended solids in raw wastewater. *Submitt. to Environ. Sci. Technol.* **2016**.

(8) Ramin, P.; Perez, B. V.; Polesel, F.; Locatelli, L.; Plósz, B. G. A systematic model identification method for chemical and biochemical transformation pathways combined with reaction kinetics – the case of heroin biomarkers. *Accepted* **2017**.